LLNL-TR-756605

Lawrence Livermore National Laboratory

The Control of an Array of Micro-mirrors

James Simonelli[1], Robert Panas[2], Jonathan B. Hopkins[1]

[1]Department of Mechanical and Aerospace Engineering
University of California, Los Angeles
Los Angeles, California, USA

[2]Lawrence Livermore National Laboratory,
P.O. Box 808, Livermore, CA 94551-0808

August 10, 2018

Disclaimer

This document was prepared as an account of work sponsored by an agency of the United States government. Neither the United States government nor Lawrence Livermore National Security, LLC, nor any of their employees makes any warranty, expressed or implied, or assumes any legal liability or responsibility for the accuracy, completeness, or usefulness of any information, apparatus, product, or process disclosed, or represents that its use would not infringe privately owned rights. Reference herein to any specific commercial product, process, or service by trade name, trademark, manufacturer, or otherwise does not necessarily constitute or imply its endorsement, recommendation, or favoring by the United States government or Lawrence Livermore National Security, LLC. The views and opinions of authors expressed herein do not necessarily state or reflect those of the United States government or Lawrence Livermore National Security, LLC, and shall not be used for advertising or product endorsement purposes.

Lawrence Livermore National Laboratory is operated by Lawrence Livermore National Security, LLC, for the U.S. Department of Energy, National Nuclear Security Administration under Contract DE-AC52-07NA27344.

Area of exploration and background

The goal of this project is to develop an array of micro electromechanical systems (MEMS) mirrors with the following characteristics: three degrees of freedom (tip, tilt, piston); ±10° range of motion; and 40kHz closed-loop bandwidth. The combination of these characteristics will push the boundaries of devices currently in the literature, enabling a myriad of applications, from glasses-less stereo imagery to high-performance beam steering.

Project goals

The UCLA team will develop and implement a method for simultaneously driving and sensing the position of the electrostatic comb drive that powers the MEMS device, enabling closed-loop control without external sensors. A model will be experimentally obtained for the comb drive paddle system (without the mirror) and will be combined with an analytical model of the decoupling flexure system to form the preliminary control design model. Simulation against this model will validate the control algorithms developed, and when the final system is ready, a grey-box model—with the structure of the control design model but with values informed by experiment—will be obtained and final control design performed. Final controller will be implemented on the prototype and experimentally verified. The UCLA team will also help improve the existing system's flexure design where necessary.

Specific tasks

The UCLA team will develop sensing implementations, models, and control strategies for the 3DOF single micromirror system. The specific tasks to be performed during this work are listed below:

1. Implement simultaneous sensing and actuation on existing paddle platform
   1.1. Develop circuitry to sense position of each comb drive
   <u>Status: Complete.</u>
   Parallel drive-sense circuitry was developed and prototyped based on a lock-in measurement on the ground return current. Current measurement was provided by a Transimpedance Amplifier (TIA) integral to the circuit and the various paddle measurements were differentiated from each other by the use of a different modulation frequency for each paddle.

   Theory of Operation:
   A high frequency (~1MHz) modulation signal was injected along with the lower-frequency drive signal to take advantage of the simultaneously low-pass (mechanical) and high-pass (electrical) frequency response of the comb drive. This ensures that the modulation signal and mechanical bandwidth are decades apart and do not interfere with each other. The return current only due to the modulation signal is $i = C\frac{dV}{dt}$ due to the capacitive nature of the comb drive actuator. When the voltage is sinusoidal, its derivative is also a sinusoid at the same frequency, effectively encoding the comb capacitance in the current as an amplitude-modulated signal. A lock-in amplifier

isolates the modulation frequency in the return current and demodulates the capacitance, which has a one-to-one correspondence with actuation angle. This capacitance can then be calibrated by an external sensor. Electrical schematics and board layout provided in Appendix.

Selected Results:

The performance of the circuitry was verified using a variable capacitor of comparable capacitance in place of the comb drive actuator, after which the best-working prototype available was tested. Due to limitations in the prototype, a full-scale test was not possible but the results obtained while working in the voltage/displacement range afforded by that prototype were promising. Experimental sensing results are summarized in Figure 1; over the range of motion available to the prototype before ill effects developed, there is good agreement between the external sensor (QPD) and the onboard sensing. A slight phase delay is observed and expected from the signal processing inherent in the lock-in measurement.

Future Work:

A disadvantage of this method is the necessity for one lock-in demodulator and one independent sinusoid generator per channel, which may limit scalability. In the prototype circuitry, only two independent channels are implemented, the sinusoids are generated in software, and the lock-in measurement is done with an external rack-

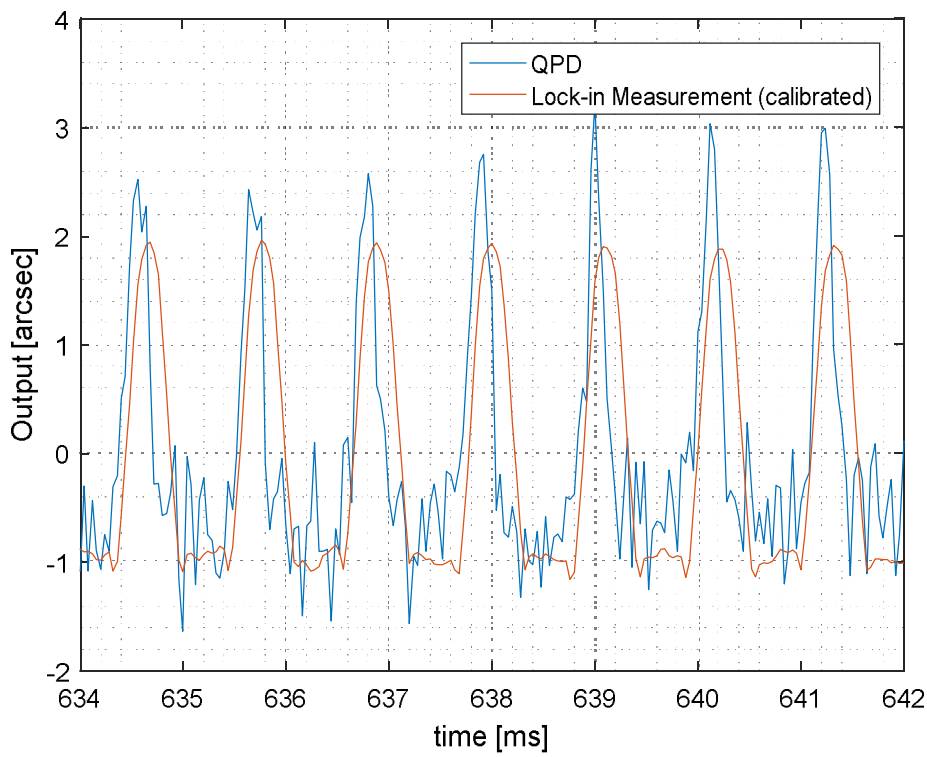

Figure 1: Small-signal Sensing Experimental Data

mounted research unit. These are all idealized conditions by comparison to the massively scaled array proposed, so on-board sine generation and carrier

demodulation must be implemented to have any chance at scaling up. It is possible to do this, but beyond the scope of this work.

1.2. Characterize sensor output, and calibrate to real-world units
<u>Status: Incomplete.</u>
Due to the unavailability of a working prototype, it was not possible to calibrate a full-scale measurement, as the prototype available could not be made to move to full scale. Calibration to the external QPD sensor was performed successfully over the limited range available, but as full-scale calibration and testing was proposed, we mark this task incomplete. Figure 1 is representative of the available range of the prototype and the performance of the sensing scheme.

1.3. Verify dynamic performance of sensing scheme
<u>Status: Incomplete</u>
Similarly, dynamic performance has been explored over a small range, but full-scale testing is yet incomplete. Figure 1 is the response of the device/sensor combination to an input sinusoid at 900Hz, which is promising, but it is not deemed useful now to further experiment on the existing prototype until a fully-operational prototype is available.

2. Develop models and control algorithms for 3DOF single micromirror system

2.1. Perform System Identification on existing paddle platform to obtain an experimental model for paddle system
<u>Status: Complete</u>
System Identification was performed on the paddle system using the electronics designed in deliverable 1.1 and sensed by the laser-QPD angle sensor developed by Ken Enstrom and duplicated on site. This provided a ground-truth measurement of the motion of the paddle; sensing was ignored for this experiment due to unavailability of a working prototype in that regard. A swept sine identification was performed on the paddle system from drive voltage [V] to angular displacement [deg] with the frequency ranging from 10Hz to 2.5 kHz, with a system sample rate of 40 kHz. A second-order linear, continuous-time model was fit to the frequency response data (FRD) obtained, and agreement between the FRD and the fit model was good. Results are summarized

in Figure 2.

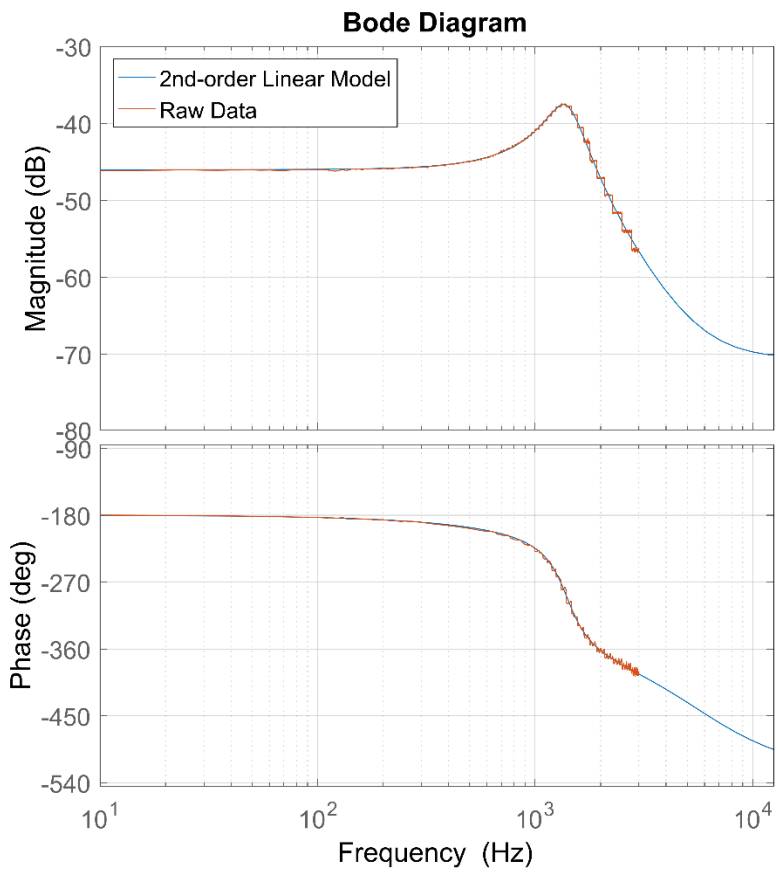

Figure 2: System Identification of a Single Paddle

2.2. Integrate with analytical/FEM model for decoupling flexures to obtain rough control design model

<u>Status: Complete</u>

An analytical model based in linear Timoshenko beam theory was constructed and implemented such that nominal geometric parameters could be input and from those parameters, a stiffness matrix for the full system could be calculated. Similarly, a mass matrix was calculated from geometric parameters and parameterized material properties, and a modified Rayleigh damping scheme was applied to obtain a damping matrix. A modal decomposition was performed on both the Mass and Stiffness matrices so that the damping of individual modes could be independently adjusted, and after appropriate scaling (based on experimental FRD obtained by Steve Hunter, the matrices were transformed back and the traditional Rayleigh Damping equation was implemented as below.

$$\mathbf{C} = \mu\mathbf{M} + \lambda\mathbf{K}$$

Agreement between the analytical model and the assembled prototype was good, and a comparison in frequency domain is given in Figure 3.

2.3. Verify control performance via simulation against this model

Status: Complete

To simulate the performance of the Micromirror under control, a standard beam-steering application was investigated. Figure 1 summarizes the simulated system; beam disturbance enters through the equivalent upstream optics, modeled as colored

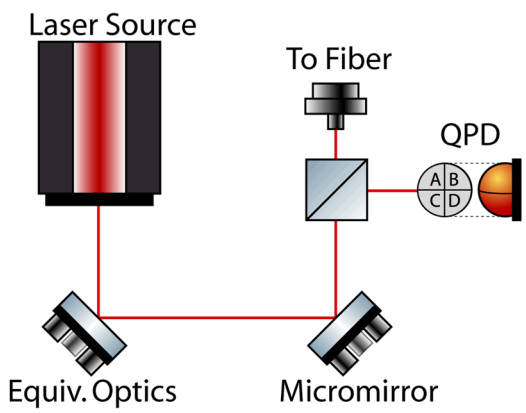

Figure 3: Simulated Beam-steering Application

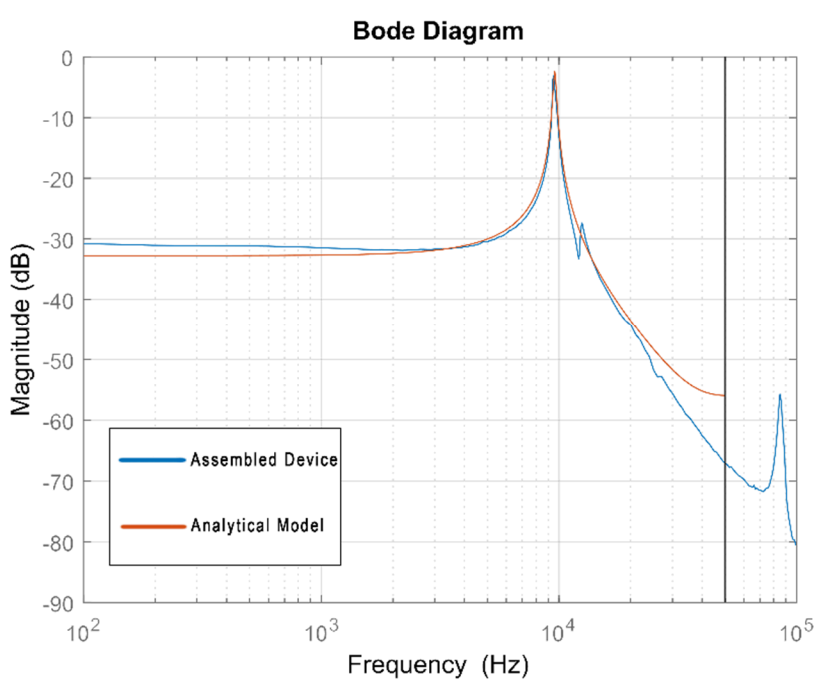

noise. The filter that generates the colored noise (and thus the approximate noise spectrum) is given in Figure 5. Three strong resonances dominate the response,

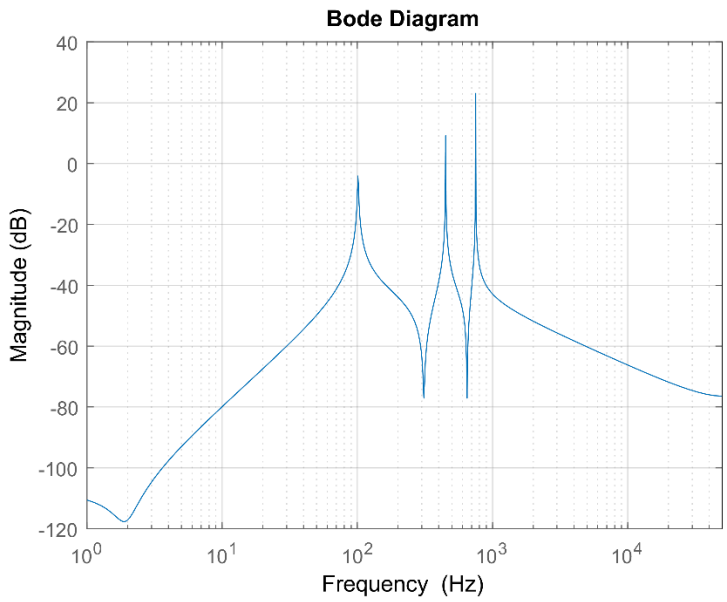

Figure 4: Simulated Disturbance Spectrum

simulating optical component/table resonances or harmonic disturbances from adjacent equipment. This disturbance is also applied to the Micromirror to simulate coupling of table vibrations into the Mirror.

The Micromirror attempts to attenuate the disturbance through a combination of ultra-high-rate feedback of the paddle angles, forward kinematic approximation of the Tip/Tilt/Piston (TTP) motion of the Mirror from the paddle angles, and lower-rate output beam position feedback from an external sensor—a quadrant photodiode (QPD) in this simulation. This leads to three nested control loops: a high-bandwidth inner loop closed on the three paddle positions, a Mirror tracking loop that commands the inner-most loop and takes a TTP reference, and an outer Adaptive regulation loop that seeks to minimize the motion of the output beam, fed back from the external sensor.

The inner-most, high-bandwidth loop consists of three independent proportional-integral (PI) control loops, each operating on a single paddle and governing the paddle angle. PI was chosen for its relative simplicity, robustness, and ease of implementation at high rates in an application-specific integrated circuit (ASIC). This allows the loop extremely high bandwidth to eliminate undesired vibrations in the paddle angles and can make full use of the high bandwidth of the Micromirror, without regard for limitations in sampling rate of available hardware. Figure 6 describes the operation of the two inner-most loops.

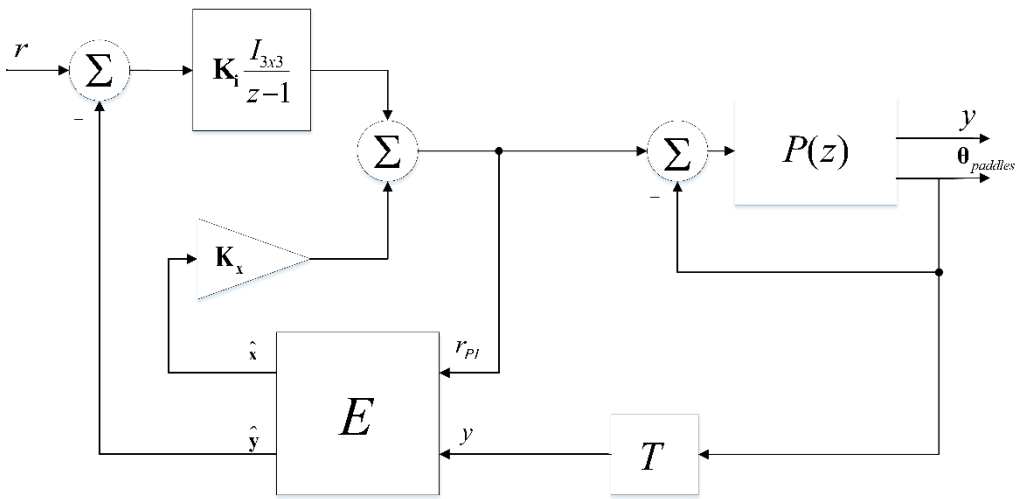

Figure 5: Inner Loops Structure

The Mirror tracking loop is the next-most inner loop, taking a TTP reference and operating on the three now-closed-loop paddles. Feedback for this loop is provided by an approximation of the Mirror TTP from forward kinematics based on the three paddle angles (denoted T in the figure). The controller is designed through Linear-Quadratic Gaussian (LQG) synthesis with integral action. An optimal controller that is inherently multi-input, multi-output (MIMO), the LQGi handles the coupling between the three inputs (paddle angles) and three outputs (TTP) and the integrator provides for tracking of references in addition to the benefits provided by the state feedback LQR controller.

The outer-most loop is the only loop to make use of the external sensor. As the disturbance is unknown *a priori*, a narrow-band controller targeted at the problem

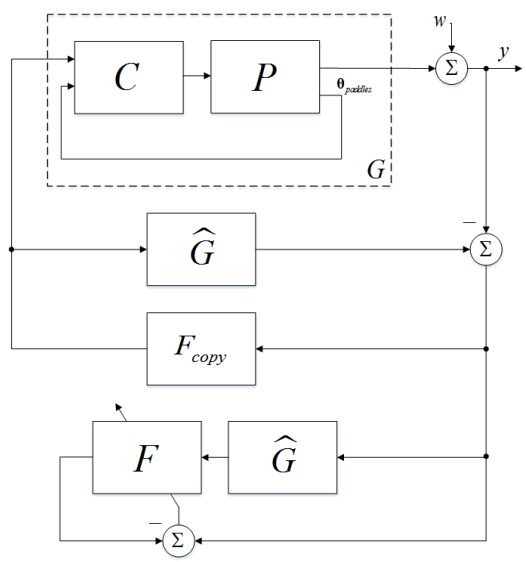

Figure 6: Adaptive Controller Structure

frequencies is infeasible, and a more broadband controller like LQGi leaves attenuation performance on the table. The solution proposed here is an adaptive controller that can

identify the unknown disturbance and allocate more control action to those problem frequencies. Figure 7 shows the adaptive controller structure [1, 2]; P denotes the

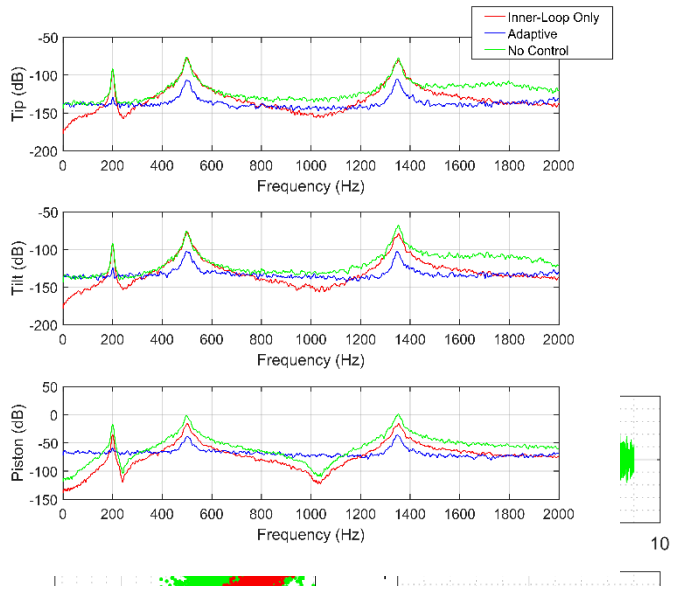

Figure 8: Frequency-Domain Combined Controller Results

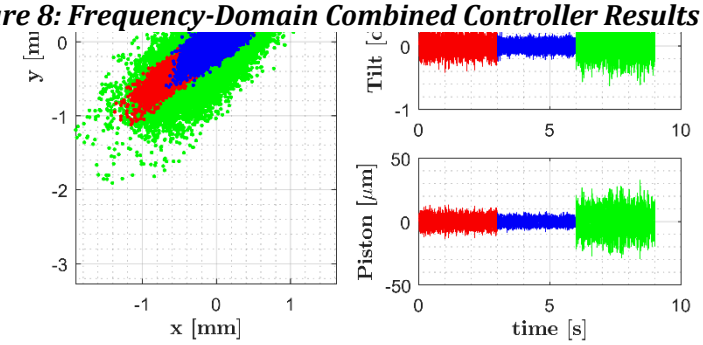

Figure 7: Time-Domain Combined Controller Results

MicroMirror analytical model, from voltages to TTP, C is the combination of the two inner loops, and $\hat{G}$ is the calculated closed-loop system resulting from those feedback loops. F is a lattice filter recursive least-squares (RLS) implementation, based on the work of Jiang and Gibson [3]. Results from the simulation of this combined control approach are given in Figures 8 and 9.

The disparity between the inner-loop controllers and the combined control strategy (marked as "Adaptive" in the figures) is clear; Figure 8 shows the error in each of the three degrees of freedom (TTP), and the resultant 2D beam path at the fiber coupling interface. The adaptive controller has a far tighter beam pattern, which is partially due to its access to the external sensor—only the external sensor can measure the disturbance on the beam before it encounters the Micromirror. The difference is clearer in Figure 9, where the error spectra are plotted. The three main harmonics are drastically attenuated by the adaptive controller, all with no *a priori* knowledge of the

trouble frequencies.

3. Experimentally verify performance of developed control strategies when final prototype available

   Status: Partially complete

   The control strategy proposed in the prior section was implemented on the available paddle prototype, making allowances for the differences between a full Mirror system and a single paddle. A PI controller was designed to close the loop on the paddle angle, and an LQGi outer-loop was designed based on the closed-loop formed by the PI controller. The nominal system $\hat{G}$ was calculated from the System ID model obtained earlier and the known controller parameters, and the adaptive controller was implemented with the laser angle sensor as feedback. Results from this experiment are given in Figure 10.

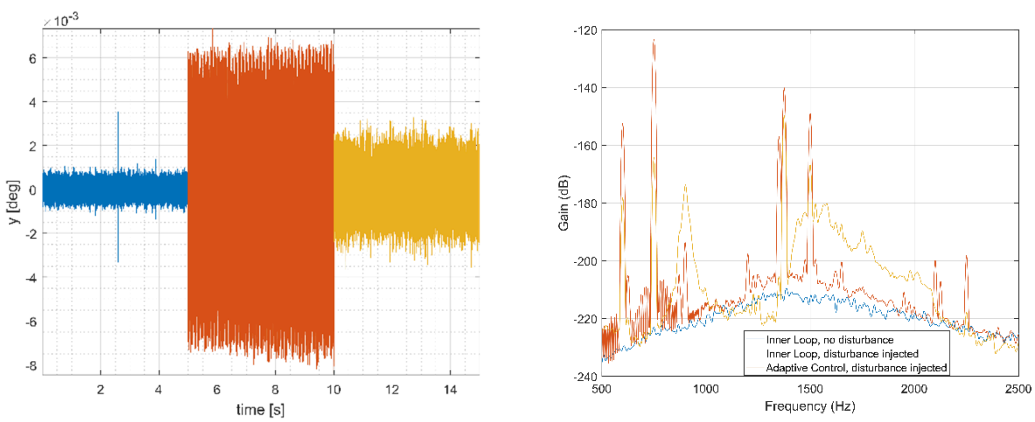

Figure 9: Experimental Control Results

As in the simulations, the three primary harmonics are attenuated by an average of 20dB. There is an issue with the amplification of certain bands by the adaptive controller that warrants further investigation, as it is not predicted by the simulation.

References

[1] Widrow, Bernard, and Eugene Walach. *Adaptive inverse control, reissue edition: a signal processing approach*. John Wiley & Sons, 2008.

[2] Chi-Ying Lin and Tsu-Chin Tsao. “Adaptive Control With Internal Model for High-Performance Precision Motion Control and Its Application to a Fast-Acting Piezoelectric Actuator.” Journal of Dynamic Systems, Measurement, and Control, 135(6):061012, 2013.

[3] Jiang, Shyh-Biau, and S. Gibson. "An unwindowed multichannel lattice filter with orthogonal channels." *IEEE Transactions on Signal Processing* 43.12 (1995): 2831-2842.